

Marquette University
e-Publications@Marquette

Chemistry Faculty Research and Publications

Chemistry, Department of

11-1-1988

Interactions of Water-soluble Metalloporphyrins with Nucleic Acids Studied by Resonance Raman Spectroscopy

Jinghua H. Schneider
Marquette University

Junichi Odo
Marquette University

Kazuo Nakamoto
Marquette University

Published version. *Nucleic Acids Research*, Vol. 16, No. 21 (November 1988): 10323-10338. [DOI](#). © 1988 Oxford University Press. Used with permission.

Interactions of water-soluble metalloporphyrins with nucleic acids studied by resonance Raman spectroscopy

Jinghua H.Schneider, Junichi Odo and Kazuo Nakamoto*

Todd Wehr Chemistry Building, Marquette University, Milwaukee, WI 53233, USA

Received June 27, 1988; Accepted September 23, 1988

ABSTRACT

The resonance Raman spectra of water-soluble porphyrins, M(TMpy-P4) (M = Cu(II), Ni(II) and Co(III)) and their mixtures with poly(dG-dC)₂, poly(dA-dT)₂ and calf thymus and salmon DNAs were measured using a divided rotating cell to determine the magnitudes of frequency shift and intensity variation resulting from M(TMpy-P4)-nucleic acid interactions. Bands II(C_α-H bending, ~1100 cm⁻¹) and VIII(C_β-C_β stretch, ~1570 cm⁻¹) show a large and small upward shift, respectively, when Cu(TMpy-P4) and Ni(TMpy-P4) are intercalated at the G-C sites. In contrast, these bands show a small upward and downward shift, respectively, when Co(TMpy-P4) is groove-bound at the A-T sites of nucleic acids. Both Bands V (~1260 cm⁻¹) and IX(~1646 cm⁻¹) which originate in the N-methylpyridyl group always show small downward shifts due to coulombic interaction between the N-CH₃⁺ group of TMpy-P4 and the PO₂ group of the nucleic acid.

INTRODUCTION

Nucleic acids interact with a variety of compounds including simple metal ions, metal complexes, antibiotics, carcinogens and biological stains. Extensive studies in the past decades have shown that basically three modes of interactions are involved in these interactions: intercalation¹, groove binding² and covalent bonding³ and that these are often reinforced by hydrogen bonding and/or coulombic interaction. The nature of drug-nucleic acid interactions has been studied extensively with a variety of physico-chemical techniques. These include x-ray crystallography, NMR, ESR, RR(resonance Raman) and IR spectroscopy. Among these, x-ray crystallography provides the most definitive and precise structural information. Unfortunately, its application is limited by the difficulties in growing single crystals of large drug-nucleic acid complexes. Recently, RR spectroscopy has been used extensively to study the structure

and bonding of large biological molecules such as heme proteins⁴ and nucleic acids⁵. In contrast to x-ray analysis, this technique is applicable to aqueous solutions under biological conditions. Furthermore, it has two distinct advantages over normal Raman spectroscopy: (1) It is possible to resonance-enhance chromophore(drug and nucleic acid) vibrations separately by tuning the laser wavelength to that of the electronic transition of each chromophore. (2) It requires only a very small volume (~ μL) of a dilute solution($10^{-3} \sim 10^{-5}$ M/L) since chromophore vibrations are enhanced by a factor of $10^4 \sim 10^5$ under resonance conditions. The purpose of our research is to exploit these advantages of RR spectroscopy for the study of porphyrin-nucleic acid interactions.

In 1979, Fiel et al.⁶ first demonstrated that the water-soluble porphyrin, $\text{H}_2(\text{TMpy-P4})$ (Fig.1), is intercalated between base-pairs of DNA. Since then, the interaction of $\text{H}_2(\text{TMpy-P4})$ and its metal derivatives with nucleic acids has been studied extensively by using gel electrophoresis⁷, CD^{8,9,10}, electronic¹⁰, fluorescence¹¹, ESR¹², NMR spectroscopy¹³, and very recently by measuring linear dichroism spectra of $\text{H}_2(\text{TMpy-P4})$ and its Zn derivative complexed to DNA in a flow gradient.¹⁴ All these studies show that $\text{H}_2(\text{TMpy-P4})$ and its Cu(II) and Ni(II) derivatives with no axial ligands intercalate at the G-C sites whereas the Zn(II), Co(III), Fe(III) and Mn(III) derivatives with axial water coordination form "outside-bound" or "groove-bound" complexes at the A-T regions of DNA^{10,15}.

Thus far, no RR studies have been made on these systems except for our preliminary work on $\text{Ni}(\text{TMpy-P4})\text{-DNA}$ ¹⁶ in spite of obvious advantages of this technique mentioned earlier. In this paper, we report the results of our RR studies on $\text{Cu}(\text{TMpy-P4})$ and its Ni(II) and Co(III) analogs mixed with $\text{poly}(\text{dG-dC})_2$, $\text{poly}(\text{dA-dT})_2$ and calf thymus and salmon sperm DNAs, and discuss the effects of intercalation and groove-binding on the RR spectra of these porphyrins. It should be noted that only the TMpy-P4 vibrations were selectively enhanced in our experiments since we employed the exciting lines in the Soret region of these metalloporphyrins.

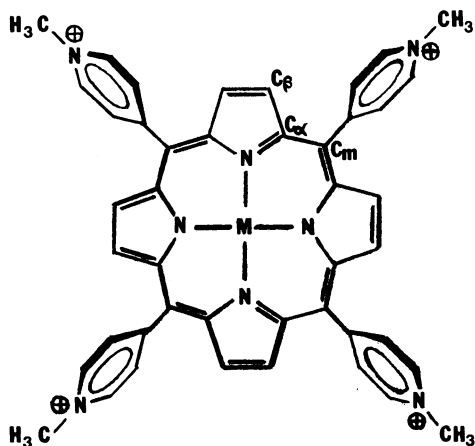


Fig. 1. Structure of M(TMpy-P4).

Recently, hematoporphyrin derivatives (HPDs) have been used for photoradiation therapy of malignant tumors¹⁷. H_2 (TMpy-P4) and its metal derivatives which can be obtained in a pure form are regarded as attractive alternatives for HPDs. In the presence of oxygen and visible light, these porphyrins can cause DNA strand scissions^{18,19}. Fe(TMpy-P4) is known to cause similar reactions in the dark.²⁰ Thus, studies on porphyrin-DNA interactions may provide structural information which is essential in understanding the roles of HPDs in photodynamic therapy.

EXPERIMENTAL SECTION

Compounds. -- The tosylate salt of the tetrakis(4-N-methylpyridyl) porphyrinato cation, [TMpy-P4]⁴⁺, was purchased from Midcentury, Posen, IL, and used without further purification. The Cu(II), Ni(II) and Co(III) complexes were prepared by published procedures¹⁰. Hereafter, these metalloporphyrin cations are abbreviated as M(TMpy-P4). Poly(dG-dC)₂ and poly(dA-dT)₂ were purchased from Pharmacia Biochemicals. Calf thymus and salmon sperm DNAs were purchased from Sigma and Pharmacia Biochemicals, respectively, and purified according to the literature method¹⁰. The DNA solution was sonicated to

shorten the average length to ca. 1,000 base pairs (determined by electrophoresis). Sample solutions were prepared by mixing aqueous solution of M(TMpy-P4) with phosphate buffer solution of nucleic acid. The final solutions thus obtained (pH = 6.8 and ionic strength = 0.2M) contained M(TMpy-P4) and nucleic acid at 10^{-5} ~ 10^{-6} and 10^{-3} ~ 10^{-4} M, respectively, as determined spectrophotometrically¹⁰. Reference solutions were prepared similarly except that the solution of a nucleic acid was replaced by the same volume of the phosphate buffer. The molar ratio(R) of base pairs/M(TMpy-P4) was kept at 20 ~ 40 unless stated otherwise.

Spectral Measurements -- Electronic spectra of both sample and reference solutions were measured on a Perkin-Elmer Model 320 UV-visible spectrophotometer. The shift and hypochromicity of the Soret band of M(TMpy-P4) resulting from interaction with nucleic acid were found to be in good agreement with those reported by Pasternack et al.¹⁰ RR spectra were measured on a Spex Model 1403 double monochromator coupled with a Spex DM1B data station. Excitations were made by using a Spectra-Physics Model 164 Kr-ion(406.7 nm), a Coherent Model 100 Kr-ion (413.1 nm), a Liconix He-Cd laser (441.6 nm) and a Spectra-Physics Model 2025 Ar-ion laser (457.9 and 476.5 nm). Both sample and reference solutions were transferred to each section of a divided rotating cell, and the RR spectra of both solutions were recorded simultaneously using a Spex difference/ratio generator. Difference spectra were obtained by subtracting the reference from the sample spectrum, and the frequency shifts were calculated by using $\Delta\tilde{\nu} = 0.385I_d\Gamma/I_0$ for $\Delta\tilde{\nu} < \Gamma$ ^{21,22,23}. Here, I_d is the peak-to-valley intensity in the Raman difference spectrum, I_0 is the intensity of the line in the Raman spectrum, and Γ is the line width. Although this equation is for Lorentzian-shaped bands, the results are approximately the same for Gaussian-shaped bands (the constant 0.385 becomes 0.350). Errors in frequency shifts thus obtained are ± 0.2 cm⁻¹(Table I) although the frequency values given in Figs. 2 to 5 are accurate within ± 1 cm⁻¹. The hypo/hyper-chromicity of RR bands plotted in the excitation profiles was calculated using the water band at 3400 cm⁻¹ as the internal standard. All the measurements were made at room temperature.

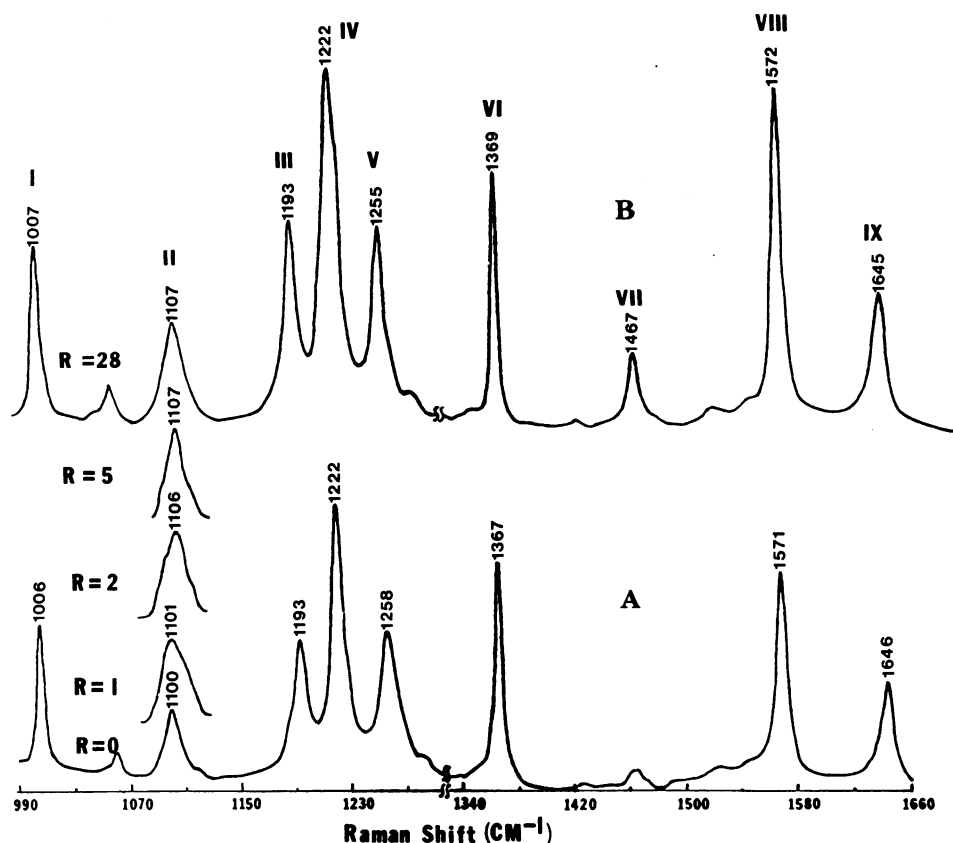


Fig. 2. RR Spectra of Cu(TMpy-P4) (trace A) and Cu(TMpy-P4) + poly(dG-dC)₂ (trace B, R = 30) (441.6 nm excitation).

Results and Discussion

Effect of Intercalation on RR Spectra of M(TMpy-P4)

As stated earlier, Cu(TMpy-P4) and Ni(TMpy-P4) are known to intercalate at the G-C sites of nucleic acids. In the latter, intercalation proceeds by losing two axial ligands (H₂O) which are present in the free state (vide infra). In order to search for marker bands for intercalation, we have compared the RR spectra of M(TMpy-P4) (M = Cu(II) and Ni(II)) and their mixtures with poly(dG-dC)₂ and DNA in buffer solution. In all these experiments, the concentration of the porphyrin was the same for the reference (M(TMpy-P4)) and the sample (M(TMpy-P4) + nucleic acid) solutions.

Table I. Band Shifts of M(TMpy-P4) Upon Interaction With Nucleic Acids(cm^{-1})

Porphyrin + Nucleic Acid	Soret Band $\Delta\lambda(\text{nm})$	%H	I $\nu(\text{C}_\alpha\text{-C}_m)$	II $\delta(\text{C}_\beta\text{-H})$	V $\nu(\text{C}_m\text{-pyr})$	VI $\nu(\text{C}_\alpha\text{-N})$	VIII $\nu(\text{C}_\beta\text{-C}_\beta)$	IX $\delta(\text{pyr})$
Cu(TMpy-P4)+ poly(dG-dC) ₂	16	35	+0.8	+6.8	-2.3	+1.6	+1.7	-0.9
Ni(TMpy-P4)+ poly(dG-dC) ₂	14	46	---	+7.3	-2.4	+0.5	+2.9	-0.6
Cu(TMpy-P4)+ calf thymus DNA	6	18	+0.7	+5.1	-2.6	+0.4	+0.4	-1.5
Ni(TMpy-P4)+ calf thymus DNA	17	38	----	+6.3	-2.5	+1.2	+0.8	-1.8
Ni(TMpy-P4)+ salmon DNA	10	42	----	+6.3	-2.3	-0.4	+0.9	-0.8
Ni(TMpy-P4)+ poly(dA-dT) ₂	6	20	----	$\sim +17.0^a$ $\sim +1.0^b$	-0.8	+0.5	-0.3	-1.8
Co(TMpy-P4)+ poly(dA-dT) ₂	5	-14	+1.9	+1.4	-1.9	-0.6	-1.8	-2.0
Co(TMpy-P4)+ calf thymus DNA	5	-27	+2.8	+2.4	-2.0	-0.5	-2.7	-2.1
Co(TMpy-P4) + poly(dG-dC) ₂	0	6	-2.3	+1.7	-1.6	-0.2	-0.1	-0.5
Cu(TMpy-P4)+ poly(dA-dT) ₂	3	-2	-1.0	+0.2	-1.5	-0.5	-0.1	-2.2

^aIt was not possible to calculate band shifts due to overlapping of two bands. a,b - Band shifts due to intercalation and groove-binding, respectively (see Text). For band assignments, see Ref. 16. ν : stretching, δ : bending.

Figure 2 shows the RR spectra (441.6nm excitation) of Cu(TMpy-P4) (trace A) and Cu(TMpy-P4) mixed with poly(dG-dC)₂ (trace B) in the 1660 - 990 cm^{-1} region. Although there are nine major bands (Bands I to IX) in this region, only six bands (Bands I, II, V, VI, VIII and IX) are discussed in this paper since Bands III and IV are only slightly sensitive to interaction with nucleic acids and since Band VII is often too weak and broad to measure the frequency shift with high accuracy. The band assignments¹⁶ of these six vibrations and their shift values together with the shift and hypochromicity¹⁰ of the Soret band are listed in Table I. Among these six bands, Band II shows the largest shift ($\sim +7 \text{ cm}^{-1}$). Figure 2 also shows the effect of changing the R value on the shape of this band. It is seen that this band is sharp and symmetrical when R=0 (no nucleic acid) and when R=28. At small R values (excess Cu(TMpy-P4)), it is broad and asymmetrical, indicating that the two bands observed at R=0 (1100 cm^{-1}) and R=28 (1107 cm^{-1}) are partially overlapped. At R>5, the peak position remains at 1107

cm^{-1} . Thus, this band is attributed to $\text{Cu}(\text{TMpy-P4})$ intercalated at the G-C site.

In aqueous solution, the four-coordinate $\text{Ni}(\text{TMpy-P4})$ exists in equilibrium mixture with the six-coordinate $\text{Ni}(\text{TMpy-P4})(\text{H}_2\text{O})_2$ with Soret band maxima located at 420 and 440 nm, respectively.^{10,16,24} Thus, the RR spectra obtained by excitation at 406.7 nm are dominated by vibrations due to the four-coordinate species, whereas the RR bands observed by 441.6 nm excitation are largely attributed to the six-coordinate species. Traces A, A' and A" of Figure 3 show the RR spectra obtained by excitation at 406.7, 413.1 and 441.6 nm, respectively. As reported previously¹⁶, Bands VI, $\nu(\text{C}_\alpha\text{-N})$, VII, $\nu(\text{C}_\alpha\text{-C}_\beta)$ and VIII, $\nu(\text{C}_\beta\text{-C}_\beta)$ are sensitive to the porphyrin core size and most useful for distinguishing four- and six coordinate species. The present result shows that Bands II ($\delta(\text{C}_\beta\text{-H})$) and I ($\nu(\text{C}_\alpha\text{-C}_m)$) are also shifted to lower frequencies in going from the four- to six-coordinate structure although their shifts are much smaller than those of the other bands. Bands III, IV, V and IX are mainly due to the N-methylpyridyl group vibrations¹⁶, and are, therefore, not sensitive to the change in coordination number of the Ni(II) atom.

When $\text{Ni}(\text{TMpy-P4})$ is intercalated to $\text{poly}(\text{dG-dC})_2$, the Soret band is shifted from 420 (four-coordinate) to 434 nm (intercalated, four-coordinate). We, therefore, compared the RR spectrum of $\text{Ni}(\text{TMpy-P4})$ (406.7 nm excitation, Fig. 3A) with that of $\text{Ni}(\text{TMpy-P4}) - \text{poly}(\text{dG-dC})_2$ (441.6 nm excitation, Fig. 3B). The observed shifts of the six marker bands are listed in Table I. These results are similar to that observed for $\text{Cu}(\text{TMpy-P4}) - \text{poly}(\text{dG-dC})_2$.

As stated earlier, $\text{M}(\text{TMpy-P4})$ ($\text{M}=\text{Cu}(\text{II})$ and $\text{Ni}(\text{II})$) intercalates at the G-C sites of nucleic acids. Pasternack et al.¹⁰ noted, however, that the reaction of $\text{Ni}(\text{TMpy-P4})$ with $\text{poly}(\text{dA-dT})_2$ results in an appreciable red shift (420 to 426 nm) and large hypochromicity (20%) of the Soret band accompanied by a conservative CD spectrum which contains both negative and positive components ($R = 30$). Figure 4 compares the RR spectrum of $\text{Ni}(\text{TMpy-P4})$ (four-coordinate, trace A) with that of $\text{Ni}(\text{TMpy-P4}) - \text{poly}(\text{dA-dT})_2$ (trace B) obtained by 413.1 nm excitation.

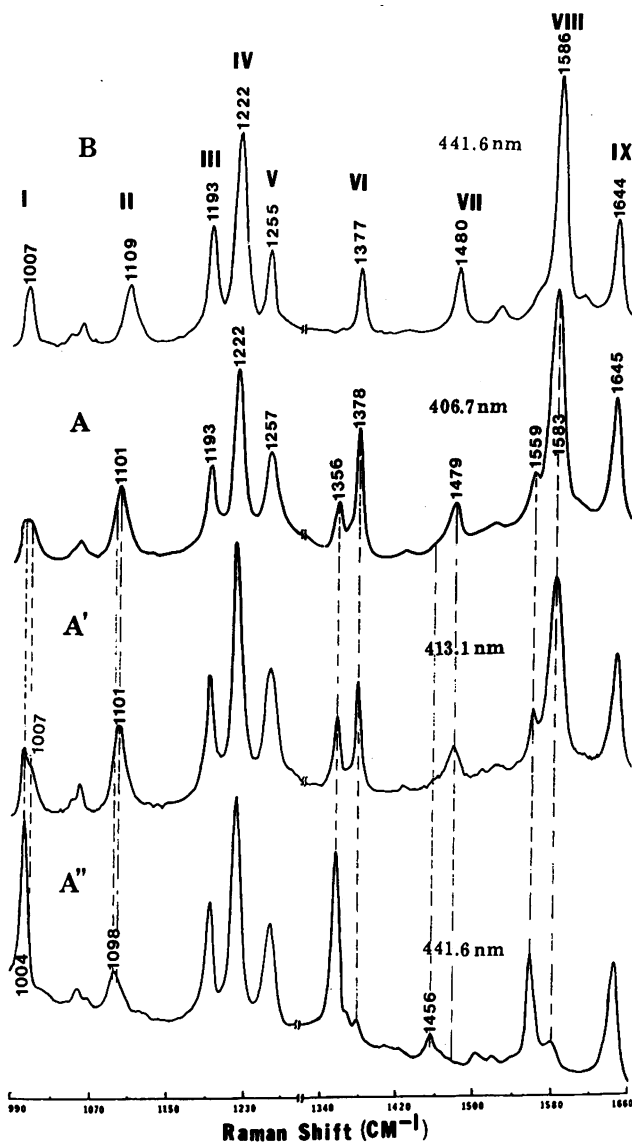


Fig. 3. RR spectra of Ni(TMpy-P4) (traces A'', A' and A by excitation at 441.6, 413.1 and 406.7 nm, respectively) and Ni(TMpy-P4)+poly(dG-dC)₂ (trace B, R=30), 441.6 nm excitation).

Table I lists the observed shifts resulting from such interaction. These shift patterns are markedly different from that of M(TMpy-P4)-poly(dG-dC)₂ (M=Cu(II) and Ni(II)).

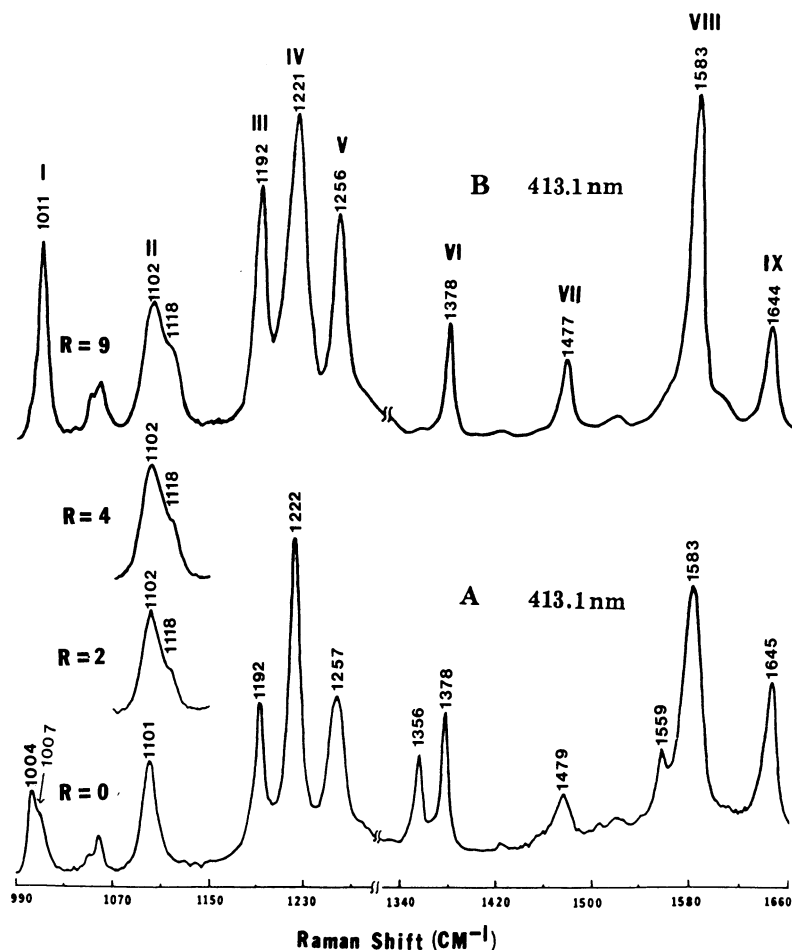


Fig. 4. RR spectra of Ni(TMpy-P4) (trace A) and Ni(TMpy-P4) + poly(dA-dT)₂ (trace B, R = 9) (413.1 nm excitation).

The most notable change resulting from Ni(TMpy-P4)-poly(dA-dT)₂ interaction occurs for Band II near 1100 cm⁻¹. As seen in the inset of Fig. 4, the sharp and symmetrical band of Ni(TMpy-P4) (four-coordinate) at 1101 cm⁻¹ becomes broader and more asymmetrical with increasing R values, and no more changes are seen after R = 9. At this R value, the main peak is centered at 1102 cm⁻¹ with a shoulder band at ~1118 cm⁻¹. Apparently, the concentration of the species responsible for the latter band increases as the relative concentration of the A-T site in-

creases. According to Pasternack et al.¹⁰, the conservative CD spectrum of Ni(TMpy-P4)-poly(dA-dT)₂ mentioned earlier may be due to the presence of two types of binding; the positive CD component results from groove-binding while the negative CD component originates in partial intercalation^{10,25}, or stacked aggregation^{8,10} along isolated regions of poly(dA-dT)₂. As will be shown later, the small shift of Band II ($\sim +1 \text{ cm}^{-1}$) is compatible with the groove-bound porphyrin. It is difficult, however, to describe the type of binding responsible for Band II at $\sim 1118 \text{ cm}^{-1}$. Possible origins of its large shift ($\sim +17 \text{ cm}^{-1}$) will be discussed in the later section.

The G-C contents of calf thymus and salmon sperm DNAs are about 41%. The RR spectra of M(TMpy-P4) (M = Cu(II) and Ni(II)) mixed with these native nucleic acids (R = 30) may be approximated as a superposition of those of M(TMpy-P4)-poly(dG-dC)₂ and M(TMpy-P4)-poly(dA-dT)₂ discussed above. Among the six bands listed in Table I, Bands II, V, VI and VIII exhibit much larger shifts for poly(dG-dC)₂ than for poly(dA-dT)₂. As a result, the shift patterns observed for M(TMpy-P4)-DNA resemble those of M(TMpy-P4)-poly(dG-dC)₂. In particular, the shift of Band II of Ni(TMpy-P4)-DNA is close to that of Ni(TMpy-P4)-poly(dG-dC)₂ and markedly different from that of Ni(TMpy-P4)-poly(dA-dT)₂. This result suggests that Ni(TMpy-P4) has a stronger GC selectivity than Cu(TMpy-P4)¹⁰.

Effect of Groove Binding on RR Spectra of Co(TMpy-P4)

As shown by Pasternack et al.¹⁰, the Zn(II), Co(III), Fe(III) and Mn(III) complexes of H₂(TMpy-P4) form groove-bound(or outside bound) complexes with nucleic acids. We have chosen the Co(III) porphyrin as the representative for our RR studies since the Zn(II) complex causes strong fluorescence background when irradiated by laser beam and since both Fe(III) and Mn(III) complexes involve pH-dependent equilibria. The Soret band of Co(TMpy-P4) at 434 nm shows no shift when mixed with poly(dG-dC)₂ and a small red shift (5 nm) when reacted with poly(dA-dT)₂. Thus, all RR spectra were obtained by using 441.6 nm excitation.

Figure 5 shows the RR spectra of Co(TMpy-P4) mixed with poly(dA-dT)₂. Table I lists the shift values of the six marker

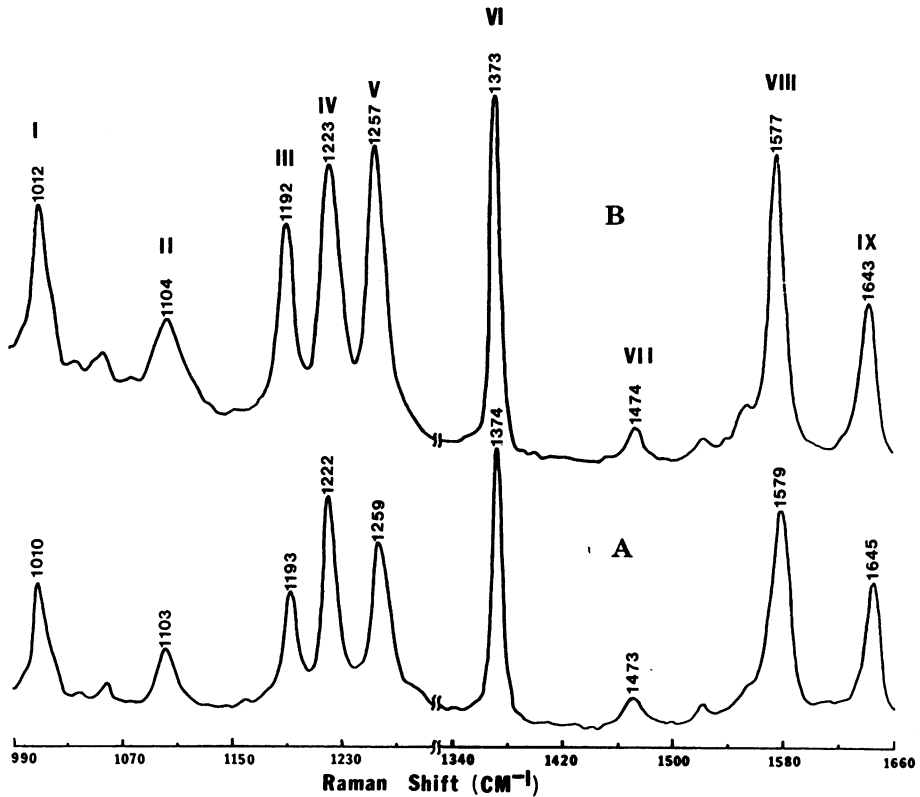


Fig. 5. RR spectra of Co(TMpy-P4) (trace A) and $\text{Co(TMpy-P4)} + \text{poly(dA-dT)}_2$ (trace B, $R = 40$) (441.6 nm excitation).

bands discussed previously. The most notable differences between this system and those of intercalated complexes are the small upward shift ($+1.4 \text{ cm}^{-1}$) of Band II and the small downward shift (-1.8 cm^{-1}) of Band VIII. Similar shift patterns are seen for Co(TMpy-P4) mixed with calf thymus DNA (Table I). Thus, we conclude that Co(TMpy-P4) is groove-bound preferentially at the A-T sites of DNA. For $\text{Co(TMpy-P4)}\text{-poly(dG-dC)}_2$ and $\text{Cu(TMpy-P4)}\text{-poly(dA-dT)}_2$, the shift patterns (Table I) are somewhat different from those of the groove-bound complexes; Band I exhibits a small downward shift and Band VIII shows almost no shift. Furthermore, these systems show no or very small shifts of the Soret band with negligible hypo/hyper-chromicity. In general, the term "outside binding" is used to indicate all

types of non-intercalative binding, namely, binding to the inside as well as the outside of the groove. Although it is rather difficult to distinguish these two types, we tentatively attribute the shift patterns observed for Cu(TMpy-P4)-poly(dA-dT)₂ and Co(TMpy-P4)-poly(dG-dC)₂ to "genuine outside binding".

Excitation Profile Studies

The hypochromicity of the Soret band is defined by $H(\%) = [(\epsilon_p - \epsilon_{bp})/\epsilon_p] \times 100$ where ϵ_p and ϵ_{bp} denote the molecular extinction coefficients of free porphyrin and bound porphyrin, respectively. Similarly, Raman hypochromicity is defined by $RH(\%) = [(I_p - I_{bp})/I_p] \times 100$, where I_p and I_{bp} denote the Raman intensities of free porphyrin and bound porphyrin, respectively. We have plotted the RH values of individual bands of Cu(TMpy-P4) complexed to poly(dG-dC)₂ as a function of the exciting laser wavelength, and compared the results with the hypochromicity curve obtained from the electronic spectra. As is shown in Fig. 6, the Raman excitation profiles thus obtained tend to follow the UV-visible hypochromicity curve. It is generally agreed that large hypochromicity of the Soret band is indicative of intercalation.¹⁰ In the case of Raman hypochromism, the degree of hypo/hyper-chromicity depends upon the wavelength of the laser beam used for excitation and the vibrational frequency of a particular normal mode. For example, Band II (~1100 cm⁻¹) is hypochromic with excitation above ~ 490 nm and below 440 nm whereas it is hyperchromic with excitation between these two regions. As is seen in Fig. 6, these threshold wavelengths are also varied slightly depending upon the vibrational frequency. Thus, Raman hypochromicity must be used with caution in determining whether a drug or porphyrin is intercalated between base pairs of nucleic acids.

Distinction of Intercalation and Groove-Binding

As summarized in Table I, RR spectra of intercalated porphyrins are characterized by large upward shifts of Band II and small upward shifts of Band VIII, whereas groove-bound porphyrins are characterized by small upward shifts of Band II and small downward shifts of Band VIII. Bands II and VIII have been assigned to the degenerate C_β - H (in-plane) bending and C_β - C_β stretching modes, respectively.¹⁶ In free M(TMpy-P4), the

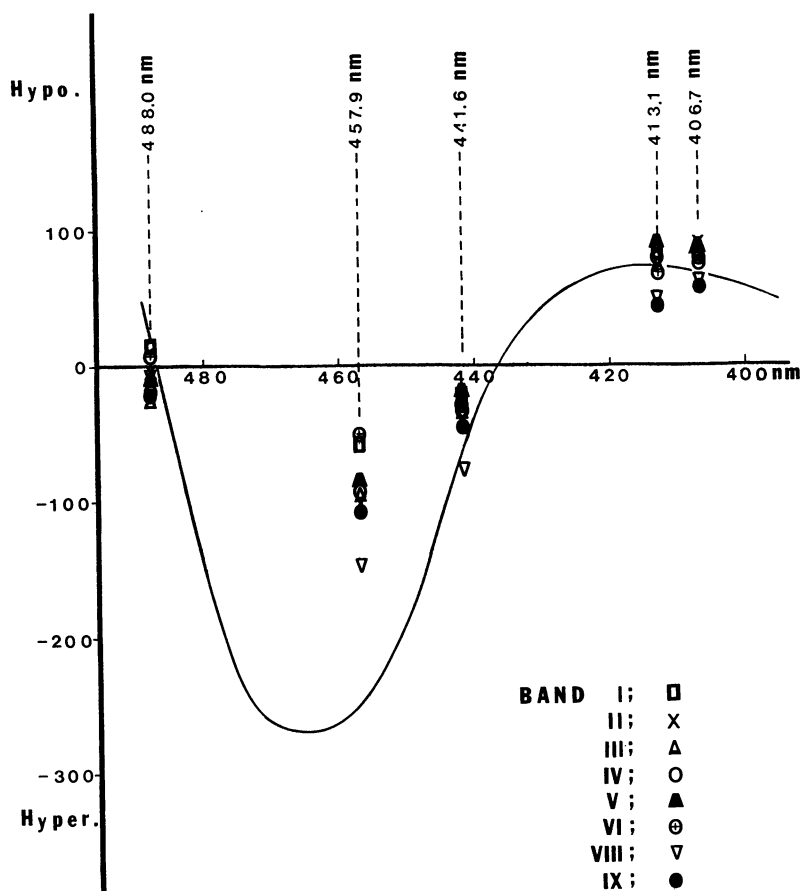


Fig. 6. UV-visible difference spectrum and RR hypochromicity profiles for Cu(TMpy-P4)-poly(dG-dC)₂ (R=30).

N-methylpyridyl(pyr) rings are nearly perpendicular to the porphyrin core plane (Fig. 1). As pointed out by Pasternack et al.¹⁰, the intercalated structure requires the rotation of the pyr ring toward the porphyrin core plane. In the case of H₂(TMpy-P2), this rotation can not occur because of the presence of the bulky N⁺-CH₃ group at the ortho position. Thus, no intercalated complexes are formed with H₂(TMpy-P2).¹⁰ Although such rotation can occur in M(TMpy-P4) (M = Cu(II) and Ni(II)), it results in severe steric hindrance for the C_β-H bending

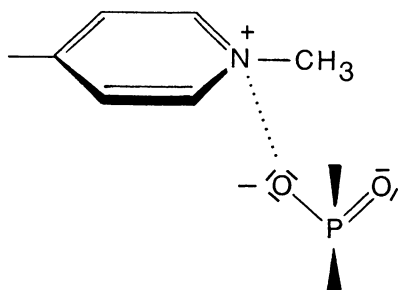


Fig. 7. Probable geometry of coulombic interaction.

vibration, thus shifting Band II to a higher frequency. The small upward shifts observed for Bands VIII, VI and I suggest that their normal modes contain some $C\beta$ -H bending character. Although the precise configuration of the M(TMpy-P4) ion in the intercalated structure is not known, Band II observed near 1108 cm^{-1} (Figs. 2 and 3) serves as the most useful marker for detecting the intercalated porphyrin. On the contrary, the rotation of the N-methylpyridyl group is not prerequisite to the groove-bound structure. In fact, Band II shows only small upward shifts ($1.5 \sim 2.5\text{ cm}^{-1}$) for Co(TMpy-P4) mixed with poly(dA-dT)₂ or calf thymus DNA.

As stated earlier, Band II of Ni(TMpy-P4)-poly(dA-dT)₂ consists of two components at 1102 and $\sim 1118\text{ cm}^{-1}$. The former band has been attributed to the groove-bound complex. However, the origin of the latter band is not certain. The observed large shift of this band ($\sim +17\text{ cm}^{-1}$) suggests that the species responsible for this band takes a structure which requires a large rotation of the pyr ring to the porphyrin core plane. It remains to be determined whether such a large rotation must occur in a partially intercalated structure^{10,25} or in a stacked aggregate along the poly(dA-dT)₂ duplex^{8,10}.

As seen in Table I, Bands V and IX always show small downward shifts regardless of the mode of interaction. The former is assigned to the degenerate C_m -pyr stretch whereas the latter is attributed to a pyr ring deformation¹⁶. Our aqueous IR studies²⁶ show that the $\nu_{as}(PO_2)$ (1223 cm^{-1}) and $\nu_s(PO_2)$ (1087 cm^{-1}) of calf thymus DNA are shifted to 1231 and 1062 cm^{-1} ,

respectively, when the DNA is mixed with Cu(TMpy-P4). We propose the presence of the coulombic interaction of the type shown in Fig. 7. In this scheme, one of the PO₂ oxygens (the P-O bond directing inside the double helix structure) interacts with the N⁺-CH₃ group, thus increasing the separation, $v_{as}(PO_2) - v_s(PO_2)$. Model building studies indicate that such interaction may occur in the intercalated as well as groove-bound porphyrin. Thus, the observed shifts of Bands V and IX are attributed to such coulombic interaction.

Finally, it should be pointed out that the porphyrin-nucleic acid system is unique in the sense that band shifts are observed because of the forced rotation of the N-methylpyridyl group in the intercalated structure and its coulombic interaction with the PO₂ groups of nucleic acids. In fact, such distinct band shifts have not been reported for Actinomycin-DNA²⁷ and Adriamycin DNA²⁸ complexes since these drugs require no appreciable conformational changes in forming intercalated structures.

Acknowledgements - This work is supported by the National Institutes of Health(GM-37608). The Raman spectrometer system used for this investigation was purchased by the National Science Foundation Grant (CHE-8413956). The authors thank Professors Robert F. Pasternack (Swarthmore College), Dennis P. Strommen (Carthage College) and Dr. Kai Bütje (Marquette University) for their valuable comments.

*To whom correspondence should be addressed.

REFERENCES

1. Wilson, W.D. and Jones, R.L. (1982) In Whittingham, M.S. and Jacobson, A.J. (eds), *Intercalation Chemistry*, Academic Press, New York, pp. 445-501.
2. Waring, M.J. (1981) *Ann. Rev. Biochem.* **50**, 159-192.
3. Jeffrey, A.M., Weinstein, I.B., Jeannette, K.W., Crzeskowiak, K. and Nakanishi, K. (1977) *Nature*, **269**, 348-350.
4. Spiro, T.G. (1983) In Lever, A.B.P. and Gray, H.B. (eds), *Iron Porphyrins*, Addison-Wesley, Reading, Massachusetts, Part II, pp. 89-159.
5. Tsuboi, M., Nishimura, Y., Hirakawa, A.Y. and Peticolas, W.L. (1987) In Spiro, T.G. (ed) *Biological Applications of*

- Raman Spectroscopy, John Wiley, New York, Vol. 2, pp. 109-179.
6. Fiel, R. J., Howard, J. C., Mark, E. H. and Datta-Gupta, N. (1979) *Nucleic Acids Res.* 6, 3093-3118.
7. Fiel, R. J. and Munson, B. R. (1980) *Nucleic Acids Res.* 8, 2835-2842.
8. Carvlin, M.J. and Fiel, R.J. (1983) *Nucleic Acids Res.* 11, 6121-6139.
9. Carvlin, M. J., Mark, E., Fiel, R. and Howard, J. C. (1983) *Nucleic Acids Res.* 11, 6141-6154.
10. Pasternack, R. F., Gibbs, E. J. and Villafranca, J. J. (1983) *Biochemistry*, 22, 2406-2414.
11. Kelly, J. M., Murphy, M. J., McConnell, D. J. and OhUigin, C. (1985) *Nucleic Acids Res.* 13, 167-184.
12. Dougherty, G., Pilbrow, J. R., Skorobogaty, A. and Smith, T. D. (1985) *J. Chem. Soc., Faraday Trans. 2*, 81, 1739-1759.
13. Marzilli, L. G., Banville, D. L., Zon, G. and Wilson, W. D. (1986) *J. Am. Chem. Soc.* 108, 4188-4192.
14. Geacintov, N. E., Ibanez, V., Rougee, M., and Bensasson, R. V. (1987) *Biochemistry*, 26, 3087-3092.
15. Pasternack, R. F., Antebi, A., Ehrlich, B., Sidney, D., Gibbs, E. J., Bassner, S. L. and Depoy, L. M. (1984) *J. Mol. Catalysis*, 23, 235-242.
16. Blom, N., Odo, J., Nakamoto, K. and Strommen, D. P., (1986) *J. Phys. Chem.* 90, 2847-2852.
17. Abstracts of the First International Conference on the Clinical Applications of Photosensitization for Diagnosis and Treatment, April 30 - May 2, 1986, Tokyo, Japan.
18. Fiel, R. J., Datta-Gupta, N., Mark, E. H. and Howard, J. C. (1981) *Cancer Res.* 41, 3543-3545.
19. Praseuth, D., Gaudemer, A., Verlhac, J.-B., Kraljic, I., Sissöeff, I., and Guillé, E. (1986) *Photochem. Photobiol.*, 44, 717-724.
20. Fiel, R. J., Beerman, T. A., Mark, E. H. and Datta-Gupta, N. (1982) *Biochem. Biophys. Res. Comm.* 107, 1067-1074.
21. Kiefer, W. (1973) *Applied Spectroscopy*, 27, 253-257.
22. Laane, J. (1981) *J. Chem. Phys.* 75, 2539-2545.
23. Shelnut, J. A. (1983) *J. Phys. Chem.* 87, 605-616.
24. Pasternack, R. F., Spiro, E.G. and Teach, M. (1974) *J. Inorg. Nucl. Chem.* 36, 599-606.
25. Ford, K., Fox, K. R., Neidle, S. and Waring, M. J. (1987) *Nucleic Acids Res.* 15, 2221-2234.
26. Nonaka, Y., Strommen, D.P., Dwivedi, A. and Nakamoto, K. to be published.
27. Chinsky, L., Turpin, P. Y., Duquesne, M. and Brahms, J. (1975) *Biochem. Biophys. Res. Comm.* 65, 1440-1446.
28. Manfait, M., Alix, A.J.P., Jeannesson, P., Jardillier, J.-C. and Theophanides, T. (1982) *Nucleic Acids Res.* 10, 3803-3816.